

Photon scattering by an atomic ensemble coupled to a one-dimensional nanophotonic waveguide

Guo-Zhu Song^{1,2}, Ewan Munro¹, Wei Nie¹, Fu-Guo Deng², Guo-Jian Yang², and Leong-Chuan Kwek^{1,3,4,5} *

¹*Centre for Quantum Technologies, National University of Singapore, 3 Science Drive 2, Singapore 117543*

²*Department of Physics, Applied Optics Beijing Area Major Laboratory,
Beijing Normal University, Beijing 100875, China*

³*Institute of Advanced Studies, Nanyang Technological University, Singapore 639673*

⁴*National Institute of Education, Nanyang Technological University, Singapore 637616*

⁵*MajuLab, CNRS-UNS-NUS-NTU International Joint Research Unit, UMI 3654, Singapore*

(Dated: March 29, 2017)

We theoretically investigate the quantum scattering of a single-photon pulse interacting with an ensemble of Λ -type three-level atoms coupled to a one-dimensional waveguide. With an effective non-Hermitian Hamiltonian, we study the collective interaction between the atoms mediated by the waveguide mode. In our scheme, the atoms are randomly placed in the lattice along the axis of the one-dimensional waveguide, which closely corresponds to the practical condition that the atomic positions can not be controlled precisely in experiment. Many interesting optical properties occur in our waveguide-atom system, such as electromagnetically induced transparency (EIT) and optical depth. Moreover, we observe that strong photon-photon correlation with quantum beats can be generated in the off-resonant case, which provides an effective candidate for producing non-classical light in experiment. With remarkable progress in waveguide-emitter system, our scheme may be feasible in the near future.

PACS numbers: 03.67.Lx, 03.67.Pp, 42.50.Ex, 42.50.Pq

I. INTRODUCTION

Since single photons have long coherent time, they are considered as the ideal candidates for quantum information processing [1]. However, the photon-photon interaction in the vacuum is very weak, and people often manipulate photons by utilizing photon-atom interaction. In the past decades, strong photon-atom interaction has been achieved by confining the photons in the high-quality optical microcavity [2, 3]. Recently, photon transport in a one-dimensional (1D) waveguide coupled to quantum emitters, known as waveguide quantum electrodynamics (QED), has been widely studied [4–26], which provides a promising candidate for realizing strong light-matter interactions. This 1D waveguide can be implemented by superconducting microwave transmission lines [27–29], surface plasmon nanowire [7], photonic crystal waveguide [30], optical nanofibers [22], and diamond waveguide [16, 31].

In 2005 and 2007, using real-space description of the Hamiltonian and the Bethe-ansatz method, Shen and Fan studied the transport properties of a single photon and two photons scattered by an emitter embedded in a 1D waveguide [4–6]. Interestingly, due to destructive quantum interference, the resonant frequency component of the photon is completely reflected by the quantum emitter. Later, several approaches are proposed to calculate single-photon transport in a 1D waveguide coupled to a two-level emitter, such as the input-output theory

[32], Lippmann-Schwinger scattering method [33], and the time-dependent theory [34]. Moreover, the scattering of a single photon by a driven Λ -type three-level emitter coupled to a 1D waveguide has been also studied [14, 18, 35]. In contrast to the single emitter case, the system composed of a single photon scattered by multiple emitters is more complicated and interesting, where quantum interference effects from multiple emitters dominates. In 2008, by solving the eigenvectors of the Hamiltonian in the single excitation subspace, Tsoi and Law [9] investigated the interaction between a single photon and a chain of N equally spaced two-level atoms inside a 1D waveguide. Later, Liao *et al.* [36] studied this system with a time-dependent theory, where many interesting phenomena occur such as Fano-like interference and photonic band-gap effects. Recently, Ewan *et al.* [37] studies the optical properties of an ensemble of two-level atoms coupled to a 1D photonic crystal waveguide.

Motivated by the important work mentioned above, we focus on the scattering property of a single photon interacting with an ensemble of Λ -type three-level atoms coupled to a 1D waveguide. Different from the previous work where the emitters are equally spaced, in our system, the atoms are randomly located in the lattice along the axis of the 1D waveguide, which closely corresponds to the experimental condition that the positions of artificial atoms can not be manipulated precisely due to inevitable technological spreading of the parameters. Since both the transmission and reflection of a single photon are fluctuant with the changeable configurations of the atomic positions and single-shot spectrum is often unavailable due to finite trap lifetimes, we take the average values from a large sample of the atomic positions.

In this paper, we first assume that the input pho-

*Corresponding author: cqtklc@nus.edu.sg

ton is a plane wave with single frequency and calculate the transport properties of a three-level atomic ensemble coupled to a 1D waveguide. Then, we consider a single photon with Gaussian shape and study the optical properties with the parameters of our system, such as the driving field, the coupling strength between atomic ensemble and the 1D waveguide, lattice constant, and the number of the atoms. It is interesting to note that our system may find application in quantum information technology, such as a single-photon frequency filter. Besides, since atoms are randomly placed in the lattice, we analyse the variance of the transmission as a function of the frequency detuning, concluding that the influence of the atomic positions on transport properties changes with frequency detuning. Finally, to probe the photon-photon correlation mediated by the ensemble of Λ -type three-level atoms, we study the second-order correlation function in off-resonant case. We find that, with strong driving field, both anti-bunching and bunching appear in the transmitted field, while only strong bunching occurs in the reflected field. Moreover, quantum beats (oscillation) [38] emerge in the photon-photon correlation function of the reflected and transmitted fields. In fact, our system provides an effective method for producing non-classical light in experiment.

The paper is organized as follows: In Sec. II, we give the model and present the derivation of the effective Hamiltonian for the system composed of an ensemble of three-level atoms and propagating photons in 1D waveguide. In Sec. III, we study the transmission and reflection of a single photon, the variance caused by the atomic positions, and photon-photon correlation in the off-resonant case. Finally, a summary is shown in Sec. IV.

II. MODEL AND HAMILTONIAN

In this section, we consider a system composed of an ensemble of Λ -type three-level atoms randomly located in a lattice of period d along the waveguide, as shown in Fig. 1. We assume that the transition with the resonance frequency ω_a between ground state $|g\rangle$ and excited state $|e\rangle$ is coupled to the mode of the 1D waveguide, and the transition $|e\rangle \leftrightarrow |s\rangle$ is driven by a classical field with the Rabi frequency Ω_c . The Hamiltonian of the full system with the rotating-wave approximation in real space reads (taking $\hbar = 1$) [4]

$$\begin{aligned}
 H = & ic \int dz \left[a_L^\dagger(z) \frac{\partial a_L(z)}{\partial z} - a_R^\dagger(z) \frac{\partial a_R(z)}{\partial z} \right] \\
 & + \sum_j^n \left[\omega_a \sigma_{ee}^j + \omega_s \sigma_{ss}^j - \Omega_c (\sigma_{es}^j e^{-i\omega_c t} + h.c.) \right] \\
 & - \tilde{g} \int dz \sum_j^n \delta(z - z_j) \{ \sigma_{eg}^j [a_R(z) + a_L(z)] + h.c. \},
 \end{aligned} \quad (1)$$

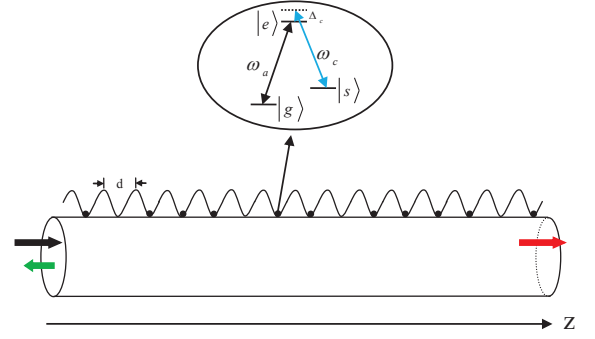


FIG. 1: Schematic diagram for the scattering of a single photon off an ensemble of Λ -type three-level atoms (black dots) coupled to a 1D waveguide (the cylinder). A photon pulse (black arrow) is input from left to interact with the atomic ensemble, which generates a transmitted part (red arrow) and a reflected part (green arrow). The wavy line denotes the lattice, and d is the lattice constant.

where a_R (a_L) denotes the the annihilation operator of right (left) propagating photon, and $\tilde{g} = \sqrt{2\pi}g$. g is the coupling strength between the atom and the waveguide mode, assumed to be identical for all the atoms. Here, we take the energy of the ground state $|g\rangle$ to be zero, and ω_s is the energy of the level $|s\rangle$. The atomic operator $\sigma_{\alpha\beta}^j = |\alpha_j\rangle\langle\beta_j|$ with $\alpha, \beta = g, e, s$ being the energy eigenstates of the j^{th} atom.

By calculating the commutators with H , we can obtain the Heisenberg equations of the motion for the atomic operators

$$\begin{aligned}
 \dot{\sigma}_{ge}^j &= -i\omega_a \sigma_{ge}^j + i\Omega_c \sigma_{gs}^j e^{-i\omega_c t} + i\tilde{g}(\sigma_{gg}^j - \sigma_{ee}^j)[a_R(z_j) + a_L(z_j)], \\
 \dot{\sigma}_{gs}^j &= -i\omega_s \sigma_{gs}^j + i\Omega_c \sigma_{ge}^j e^{i\omega_c t} - i\tilde{g}\sigma_{es}^j[a_R(z_j) + a_L(z_j)], \\
 \dot{\sigma}_{es}^j &= i\omega_c \sigma_{es}^j + i\Omega_c(\sigma_{ee}^j - \sigma_{ss}^j)e^{i\delta t} - i\tilde{g}\sigma_{gs}^j[a_R^\dagger(z_j) + a_L^\dagger(z_j)].
 \end{aligned} \quad (2)$$

Using the same method, we can also write the Heisenberg equations of the motion for the photons

$$\begin{aligned}
 \left(\frac{1}{c} \frac{\partial}{\partial t} + \frac{\partial}{\partial z}\right) a_R(z) &= \frac{i\tilde{g}}{c} \sum_j^n \delta(z - z_j) \sigma_{ge}^j, \\
 \left(\frac{1}{c} \frac{\partial}{\partial t} - \frac{\partial}{\partial z}\right) a_L(z) &= \frac{i\tilde{g}}{c} \sum_j^n \delta(z - z_j) \sigma_{ge}^j.
 \end{aligned} \quad (3)$$

Then, the Heisenberg equations for a_R (a_L) can be integrated, and we get the real-space wave equation

$$\begin{aligned}
 a_R(z, t) &= a_{R,in}(z - ct) + \frac{i\tilde{g}}{c} \sum_j \theta(z - z_j) \sigma_{ge}^j \left(t - \frac{z - z_j}{c}\right), \\
 a_L(z, t) &= a_{L,in}(z + ct) + \frac{i\tilde{g}}{c} \sum_j \theta(z_j - z) \sigma_{ge}^j \left(t - \frac{z_j - z}{c}\right).
 \end{aligned} \quad (4)$$

Here, the first term $a_{R,in}$ ($a_{L,in}$) represents the freely traveling field in the waveguide, while the second term

corresponds to the contribution of the field emitted by the atomic ensemble. Since we are more interested in the scattered field induced by atoms, here we set $a_{R,in} = a_{L,in} = 0$. Inserting the above field equation into the Eq. (2), we can get the equation for the atoms alone

$$\begin{aligned}\dot{\sigma}_{ge}^j &= -i\omega_a\sigma_{ge}^j + i\Omega_c\sigma_{gs}^j e^{-i\omega_c t} \\ &\quad - \frac{\tilde{g}^2}{c}(\sigma_{gg}^j - \sigma_{ee}^j) \sum_{k \neq j} \sigma_{ge}^k(t - \frac{|z_j - z_k|}{c}), \\ \dot{\sigma}_{gs}^j &= -i\omega_s\sigma_{gs}^j + i\Omega_c\sigma_{ge}^j e^{i\omega_c t} \\ &\quad + \frac{\tilde{g}^2}{c}\sigma_{es}^j \sum_{k \neq j} \sigma_{ge}^k(t - \frac{|z_j - z_k|}{c}), \\ \dot{\sigma}_{es}^j &= i\omega_c\sigma_{es}^j + i\Omega_c(\sigma_{ee}^j - \sigma_{ss}^j)e^{i\omega_c t} \\ &\quad - \frac{\tilde{g}^2}{c}\sigma_{gs}^j \sum_{k \neq j} \sigma_{eg}^k(t - \frac{|z_j - z_k|}{c}).\end{aligned}\quad (5)$$

Then, by transforming to the slow-varying frame, we can define the three following quantities:

$$\begin{aligned}\sigma_{ge}^j(t) &= S_{ge}^j(t)e^{-i\omega_{in}t}, \quad \sigma_{gs}^j(t) = S_{gs}^j(t)e^{-i(\omega_{in}-\omega_c)t}, \\ \sigma_{es}^j(t) &= S_{es}^j(t)e^{i\omega_c t},\end{aligned}\quad (6)$$

where ω_{in} is the frequency of the incident photon pulse.

When the atomic resonance frequency ω_a is far away from the cutoff frequency of the waveguided mode, and the photon has a narrow bandwidth in vicinity of ω_a , we can adopt the linear dispersion approximation [39]. Using this condition, Eq. (5) is rewritten as

$$\begin{aligned}\dot{S}_{ge}^j &= i\Delta S_{ge}^j + i\Omega_c S_{gs}^j \\ &\quad - \frac{\Gamma_{1D}}{2}(S_{gg}^j - S_{ee}^j) \sum_{k \neq j} S_{ge}^k(t)e^{ik_{in}|z_j - z_k|}, \\ \dot{S}_{gs}^j &= i(\Delta - \Delta_c)S_{gs}^j + i\Omega_c S_{ge}^j \\ &\quad + \frac{\Gamma_{1D}}{2}S_{es}^j \sum_{k \neq j} S_{ge}^k(t)e^{ik_{in}|z_j - z_k|}, \\ \dot{S}_{es}^j &= i\Omega_c(S_{ee}^j - S_{ss}^j) - \frac{\Gamma_{1D}}{2}S_{gs}^j \sum_{k \neq j} S_{eg}^k(t)e^{ik_{in}|z_j - z_k|},\end{aligned}\quad (7)$$

where $\Delta = \omega_{in} - \omega_a$, and $\Gamma_{1D} = 2\tilde{g}^2/c$. $\Delta_c = \omega_c - \omega_{es}$ is the frequency detuning between the driving field and the transition $|s\rangle \rightarrow |e\rangle$. From the above equations, after eliminating the fields, we can get an effective Hamiltonian for the system

$$\begin{aligned}H_{eff} &= -\sum_j^n [\Delta S_{ee}^j + (\Delta - \Delta_c)S_{ss}^j] - \Omega_c \sum_j^n [(S_{es}^j + S_{se}^j)] \\ &\quad - i\frac{\Gamma_{1D}}{2} \sum_{j,k} e^{ik_{in}|z_j - z_k|} S_{eg}^j S_{ge}^k.\end{aligned}\quad (8)$$

In the spirit of the quantum jump, spontaneous emission into free space other than the waveguide can be

modeled by attributing an imaginary part $-i\Gamma'/2$ to the energies of the states of the atoms [40]. Therefore, the whole system composed of the atomic ensemble and the 1D waveguide can be described by an effective non-Hermitian Hamiltonian

$$\begin{aligned}H &= -\sum_j^n [(\Delta + i\Gamma'_e/2)S_{ee}^j + (\Delta - \Delta_c + i\Gamma'_s/2)S_{ss}^j \\ &\quad + \Omega_p(S_{eg}^j e^{ik_{in}z_j} + h.c.)] - \Omega_c \sum_j^n [(S_{es}^j + S_{se}^j)] \\ &\quad - i\frac{\Gamma_{1D}}{2} \sum_{j,k} e^{ik_{in}|z_j - z_k|} S_{eg}^j S_{ge}^k,\end{aligned}\quad (9)$$

where Ω_p is the Rabi frequency of the input probe field, z_j is the position of the j^{th} atom, and Γ'_e (Γ'_s) is the decay rate of the state $|e\rangle$ ($|s\rangle$) into the free space.

Here, since we focus mainly on the reflection and transmission of a weak probe field ($\Omega_p/\Gamma'_e \ll 1$), the quantum jumps give a vanishing contribution and can be neglected. Provided that all atoms are in the ground states $|g\rangle$ and a photon pulse is coming from the left with the wavevector k_{in} , with the input-output methods [41], we can obtain the transmitted (T) and reflected (R) fields

$$\begin{aligned}a_{out,T}(z) &= \Omega_p e^{ik_{in}z} + \frac{i\Gamma_{1D}}{2} \sum_j S_{ge}^j e^{ik_{in}(z-z_j)}, \\ a_{out,R}(z) &= \frac{i\Gamma_{1D}}{2} \sum_j S_{ge}^j e^{-ik_{in}(z-z_j)},\end{aligned}\quad (10)$$

where the transmitted (reflected) field is defined for $z > z_R \equiv \max[z_i]$ ($z < z_L \equiv \min[z_i]$). In fact, the optical properties of the output field are determined by the input field and the dynamics of the atom-waveguide system alone. Therefore, the reflection of a single-photon pulse for the steady-state is calculated by

$$R = \frac{\langle \psi | a_R^\dagger a_R | \psi \rangle}{\Omega_p^2},\quad (11)$$

where $|\psi\rangle$ is the steady-state wavevector. For the transmitted field, the equation is similar.

III. RESULTS

A. The transmission and reflection of a single photon

The quantum interference of a single-photon scattering with a chain of atoms inside a 1D waveguide has been studied in the previous work [9, 36, 42]. In their calculations, the atoms are equally spaced with a deterministic separation d , which can be solved by the Bethe-ansatz approach [9], the transfer matrix method [42], and time-dependent dynamical theory [36]. In this section,

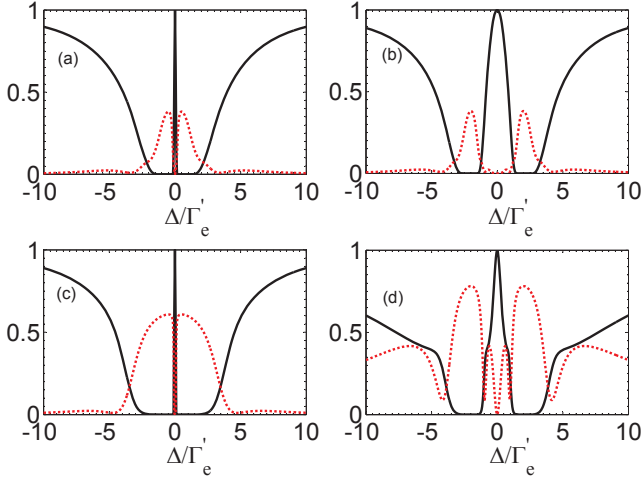


FIG. 2: Single-photon transmission T (black solid line) and reflection R (red dotted line) as a function of incident photon detuning in two cases. Here, one case is that $n = 10$ atoms are placed in a lattice of $N = 10$ sites, i.e., 10 atoms are equally spaced with (a) $\Omega_c = 0.5\Gamma'_e$, (b) $\Omega_c = 2\Gamma'_e$. The other case is that $n = 10$ atoms are randomly placed in a lattice of $N = 200$ sites with (c) $\Omega_c = 0.5\Gamma'_e$, (d) $\Omega_c = 2\Gamma'_e$. Parameters: (a)-(d) $\Omega_p = 0.001\Gamma'_e$, $\Gamma_{1D} = 2\Gamma'_e$, $\Gamma'_s = 0$, $k_{in}d = \pi/2$, and $\Delta_c = 0$.

assuming that the photon is a plane wave with single frequency, we study the scattering spectrum for $n=10$ three-level atoms randomly placed in a lattice of $N=200$ sites. For comparison, we first give the transmission and reflection of a single photon traveling through 10 equally spaced three-level atoms, as shown in Figs. 2(a)-(b). While, when 10 atoms are randomly placed in a lattice of $N=200$ sites, the results are quite different, and the calculations for one possible configuration of atomic positions are shown in Figs. 2(c)-2(d). In fact, the scattering property of a single photon is influenced by the atomic positions.

In Figs. 3(a)-(b), we plot the transmission and reflection of the incident probe photon with detuning Δ/Γ'_e for different values of the control beam Rabi frequency Ω_c , averaged over 1000 samples of atomic positions. First, we consider the case that the levels $|g\rangle$ and $|s\rangle$ are two hyperfine states in the ground state manifold, where the level $|s\rangle$ is metastable and $\Gamma'_s=0$. We observe that the atomic ensemble becomes fully transparent when the detuning is zero in the presence of the control field, which is known as EIT [43]. In fact, this phenomenon derives from destructive interference between two allowed atomic transitions, which causes the cancellation of the population of the excited state $|e\rangle$. As shown in Figs. 3(c)-(d), we calculate the width w of the central transparency window near two-photon resonance. Here, the width w of the EIT window is defined by $T=T_{\Delta=0}\exp(-\Delta^2/w^2)$ [44], which only holds for small Δ . We observe that the width of the EIT window is proportional to the parameters Ω_c^2/Γ_{1D} and $\frac{1}{\sqrt{n}}$, which agrees with the results of the one atom case [45] and linear array of superconducting

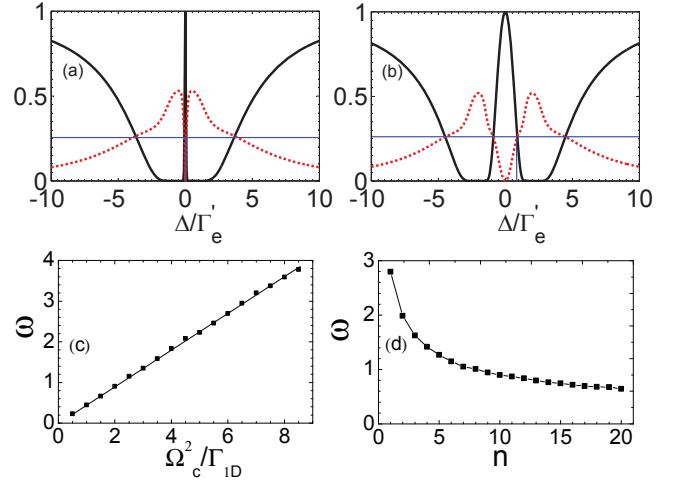


FIG. 3: Single-photon average transmission T (black solid line) and reflection R (red dotted line) as a function of incident photon frequency detuning for (a) $\Omega_c = 0.5\Gamma'_e$, (b) $\Omega_c = 2\Gamma'_e$. The width w of the EIT window as a function of the parameter (c) Ω_c^2/Γ_{1D} , and the number of the atoms (d) n . (a)-(c) $n=10$ atoms are randomly placed in a lattice of $N=200$ sites, (d) $N=200$, $\Omega_c = 2\Gamma'_e$. (a)-(d) we average over 1000 samples of atomic positions with $\Omega_p = 0.001\Gamma'_e$, $\Gamma_{1D} = 2\Gamma'_e$, $\Gamma'_s = 0$, $k_{in}d = \pi/2$, and $\Delta_c = 0$.

artificial atoms [42]. While, different from single three-level atom case [35, 45], we see that the transmission is zero in two regions of the frequency detuning on either side of the central transparency window, and the optical depth is the result of the scattering of multiple atoms. In fact, by controlling the coupling strength Γ_{1D} and the number of the atoms n , we can tune the bandwidth.

We also study the influence of different values of Γ'_s on the transmission and reflection spectra of the driven Λ -type atomic ensemble. As shown in Fig. 4, different values of Γ'_s have remarkable effect on both transmission and reflection. We observe that only when the level $|s\rangle$ is metastable, i.e., $\Gamma'_s=0$, the atomic ensemble coupled to 1D waveguide can be fully transparent on resonance, as shown in Fig. 4(a). Furthermore, with the increase of Γ'_s , the values of the peaks in transmitted spectrum decrease, and finally the EIT transparency window disappears. Interestingly, with a low decay rate Γ'_s , the reflection on resonance is always zero, while, when Γ'_s is large enough, the reflection on resonance turns to be nonzero, as shown in Figs. 4(c)-4(d).

B. Single-photon with Gaussian shape

In practice, the photon is a pulse with finite bandwidth. Here, we study the scattering property of a Gaussian pulse interacting with atomic ensemble coupled to a 1D waveguide. In experiment, using a single-photon electric-optic modulation [46], we can produce a single-

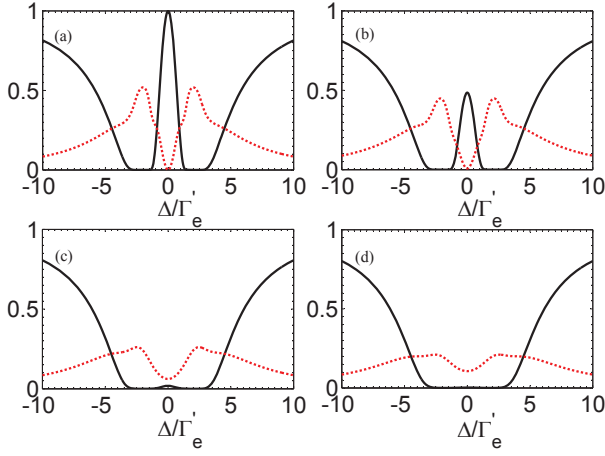


FIG. 4: Single-photon transmission T (black solid line) and reflection R (red dotted line) as a function of incident photon detuning for different values of the parameter Γ'_s . Parameters: (a) $\Gamma'_s=0$, (b) $\Gamma'_s=0.3\Gamma'_e$, (c) $\Gamma'_s=2\Gamma'_e$, (d) $\Gamma'_s=3.5\Gamma'_e$. Here, $n=10$ atoms are randomly placed in a lattice of $N=200$ sites, and we average over 1000 samples of atomic positions and set the parameters $\Omega_p=0.001\Gamma'_e$, $\Gamma_{1D}=2\Gamma'_e$, $\Omega_c=2\Gamma'_e$, $k_{in}d=\pi/2$, and $\Delta_c=0$.

photon pulse with Gaussian shape given by

$$A(\omega) = \frac{(8\pi)^{\frac{1}{4}}}{\sqrt{\sigma L}} e^{-(\omega-\omega_0)^2/\sigma^2}, \quad (12)$$

where σ is the width in the frequency space with the full width at half maximum of the spectrum, L is the quantization length in the propagation direction, and ω_0 is the center frequency of the pulse.

As shown in Fig. 5(a), we calculate the spectrum of the photon before and after the interaction with atomic ensemble when $\omega_0 = \omega_a$, $\Omega_c = 2\Gamma'_e$, and $\Gamma_{1D} = 2\Gamma'_e$. We observe that the spectrum of transmitted photon is similar to the initial shape of the incident photon and the photon component around the atomic resonant frequency ω_a can transmit the atomic ensemble completely, while the reflected component is quite different and has two peaks. However, when we turn the condition $\Omega_c=2\Gamma'_e$ into $\Omega_c=0.5\Gamma'_e$ with other parameters remaining unchanged, we can get different results shown in Fig. 5(b): the width of the transmitted spectrum becomes small and the values of the peaks in the spectrum of the reflected part turns large. From the calculations mentioned above, we can conclude that when $\frac{\Omega_c}{\Gamma'_e} \gg 1$, the shape of the transmitted photon is very similar to the input photon, while when $\frac{\Omega_c}{\Gamma'_e} \ll 1$, a Lorentzian peak appears at the frequency $\omega = \omega_a$ in the spectrum of the transmitted pulse, which is actually the result of EIT shown in Fig. 3.

The spectra of the transmitted photons with different numbers of atoms under the condition $\omega_0 = \omega_a$, $\Omega_c = 0.5\Gamma'_e$, and $\Gamma_{1D} = 2\Gamma'_e$ are shown in Fig. 5(c). Here, four cases are considered: $n=5$ (red), 10 (blue), 20 (green), 50 (yellow) atoms are randomly placed in a lattice of $N=200$ sites, and we average over 1000 samples of

atomic positions for every case. We see that, when more atoms are placed in the lattice, the Lorentzian peak in the spectrum of the transmitted photon becomes narrower. Moreover, we study a more general case where the center frequency ω_0 of the incident Gaussian pulse is different from atomic resonant frequency ω_a . For example, the transmitted spectrum under the condition $\omega_0 = \omega_a - 0.5\Gamma'_e$ is shown in Fig. 5(d). Although $\omega_0 \neq \omega_a$, the number of the atoms has the same effect on the spectrum, i.e., the component of the single photon at the resonant frequency can also transmit the atomic ensemble completely. As shown in Figs. 5(a)-(d), by tuning the strength of the driving field and the number of the atoms, we can only transmit the frequency component ω_a of the Gaussian pulse completely, and the other parts of the Gaussian pulse will be reflected or decay into the free space. That is, our system may be useful as a single-photon frequency filter.

The reflection, transmission, and loss as a function of coupling strength under the condition $\Omega_c = 2\Gamma'_e$ are shown in Fig. 5(e). We see that the transmission (reflection) of the Gaussian pulse decreases (increases) when we increase the coupling strength Γ_{1D} , while the loss first increases and then decreases to a deterministic value (not zero) as we enhance the coupling strength. When $\Gamma_{1D} \approx 5.75\Gamma'_e$, the loss of the single-photon pulse reaches the maximum value 19.7%. However, as we only change the condition $\Omega_c = 2\Gamma'_e$ to be $\Omega_c = 0.5\Gamma'_e$, the calculations are different, as shown in Fig. 5(f). We observe that the variation trends of the reflection, transmission, and loss with the coupling strength are the same, while they all change more rapidly than the results with $\Omega_c = 2\Gamma'_e$. In this case, with $\Gamma_{1D} \approx 0.5\Gamma'_e$, we get the maximum value of loss about 69.0%. Moreover, the transmission will approach zero when the coupling strength is large enough in both cases.

We also study the transmission as a function of the detuning between the center frequency ω_0 of the incident Gaussian pulse and atomic resonant frequency ω_a . The calculations are shown in Fig. 5(g), where we consider three choices of the driving fields. In the three cases, i.e., the driving field $\Omega_c = 0.5\Gamma'_e, 1\Gamma'_e, 2\Gamma'_e$, the similarities are: (1) a peak appears at the frequency $\omega_0 = \omega_a$ in the transmitted spectrum, which is actually the result of EIT, (2) two dips exist when the center frequency of the Gaussian pulse is red and blue detuned from the atomic resonant frequency, (3) the transmission of the Gaussian pulse will approach 1 when ω_0 is far detuned from ω_a , which corresponds to the fact that the single-photon pulse will transmit the atomic ensemble with no interaction when $(\omega_0 - \omega_a) \gg \Gamma'_e$. However, with different choices of the driving fields, the values of the peaks at the frequency $\omega_0 = \omega_a$ are quite different. When the Rabi frequency of the driving field is $\Omega_c = 2\Gamma'_e$, the value of the peak can be 75.9%, while, if it is changed to be $\Omega_c = 1\Gamma'_e$ ($0.5\Gamma'_e$), the value of the peak drops down to 30.2% (8.2%), which are consistent with the results shown in Figs. 3(a)-(b). Therefore, to effectively control the transmission of the

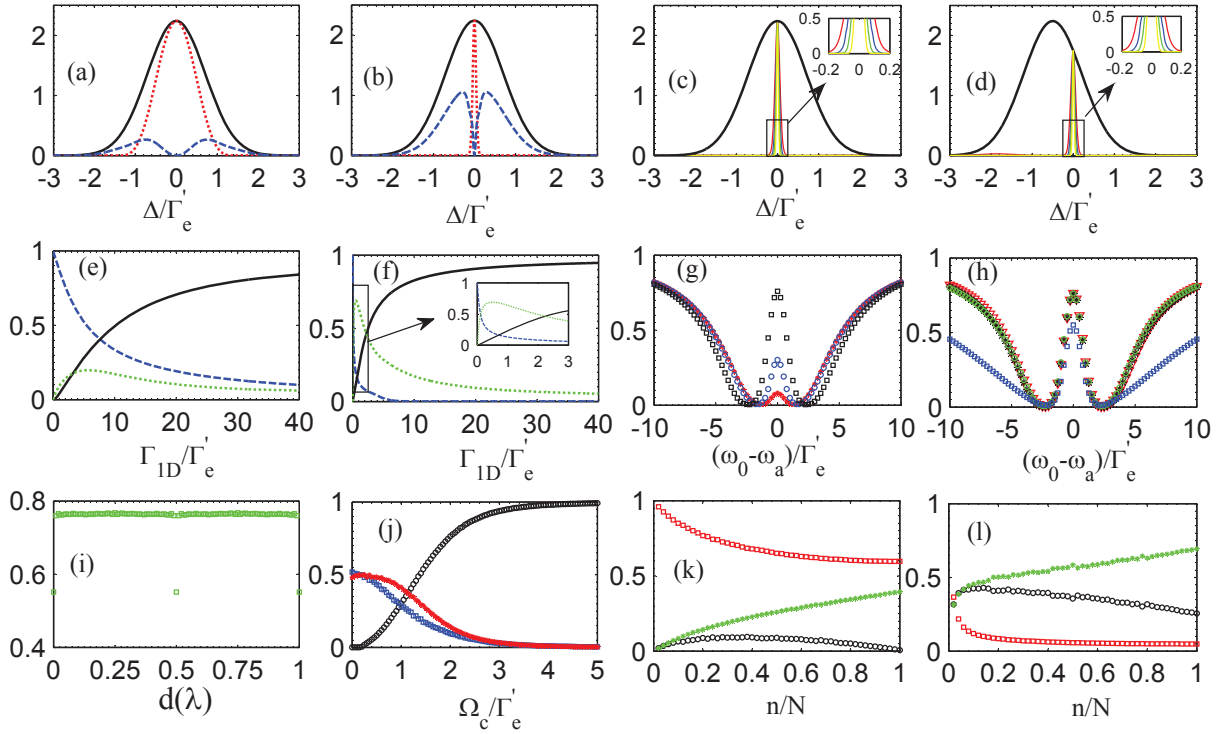


FIG. 5: The pulse shapes of the incident (black solid line), reflected (blue dashed line), and transmitted (red dotted line) photons with (a) $\Omega_c = 2\Gamma'_e$, and (b) $\Omega_c = 0.5\Gamma'_e$. The pulse shapes of the incident (black), and transmitted photons for $n=5$ (red), 10 (blue), 20 (green), 50 (yellow) atoms randomly placed in a lattice of $N=200$ sites with $\Omega_c = 0.5\Gamma'_e$, (c) $\omega_0 = \omega_a$, and (d) $\omega_0 = \omega_a - 0.5\Gamma'_e$. The reflection (black solid line), transmission (blue dashed line), and loss (green dotted line) as a function of the coupling strength Γ_{1D}/Γ'_e with (e) $\Omega_c = 2\Gamma'_e$, and (f) $\Omega_c = 0.5\Gamma'_e$. (g) The transmission as a function of center frequency deviation for different driving fields $\Omega_c = 0.5\Gamma'_e$ (red asterisks), $\Omega_c = 1.0\Gamma'_e$ (blue circles), and $\Omega_c = 2\Gamma'_e$ (black squares). (h) The transmission as a function of center frequency deviation for different lattice constant $k_{in}d = \pi$ (blue squares), $k_{in}d = 0.75\pi$ (green circles), $k_{in}d = 0.5\pi$ (black asterisks), and $k_{in}d = 0.25\pi$ (red down triangles) with $\Omega_c = 2\Gamma'_e$. (i) The transmission as a function of lattice constant d with $\Omega_c = 2\Gamma'_e$. (j) The transmission (black circles), reflection (blue squares) and loss (red asterisks) as a function of the driving fields Ω_c/Γ'_e . The transmission (red squares), reflection (black circles), and loss (green asterisks) as a function of the filling factor n/N with (k) $\Omega_c = 2\Gamma'_e$, and (l) $\Omega_c = 0.5\Gamma'_e$. Parameters: (a)-(l) we average over 1000 samples of atomic positions with the parameters $\Gamma'_s = 0$, $\Delta_c = 0$ and $\Omega_p = 0.001\Gamma'_e$, (a)-(g) and (i)-(l) $k_{in}d = \pi/2$, (a)-(d) and (g)-(l) $\Gamma_{1D} = 2\Gamma'_e$, (a)-(b), (e)-(f), and (i)-(l) $\omega_0 = \omega_a$, (a)-(b) and (e)-(j) $n = 10$ atoms are randomly placed in a lattice of $N = 200$ sites, (k)-(l) the number of the sites in the lattice is $N = 50$.

incident Gaussian pulse, one way is changing the driving field, and the other way is changing the center frequency ω_0 of the Gaussian pulse. Furthermore, the transmission as a function of the detuning $(\omega_0 - \omega_a)$ for different choices of $k_{in}d$ is shown Fig. 5(h). When $k_{in}d = 0.25\pi$, $k_{in}d = 0.5\pi$, and $k_{in}d = 0.75\pi$, the shapes of functions are very similar. However, with $k_{in}d = \pi$, for almost the whole region of the detuning $(\omega_0 - \omega_a)$, the transmission of the Gaussian pulse becomes smaller than those in the three cases mentioned above. To show clearly the influence of lattice constant d on the transmission of the Gaussian pulse, we plot the Fig. 5(i) with $\Omega_c = 2\Gamma'_e$. An obvious difference appears in the transmission when the lattice constant is $d = 0, \lambda/2, \lambda$, respectively. While, for any other choices of d , the values of the transmission are basically the same. In fact, this phenomenon is caused by the last part of the Hamiltonian in Eq. (9). In the

three special cases $d = 0, \lambda/2, \lambda$, for any possible configurations of atomic positions, the imaginary component of $e^{ik_{in}|z_j - z_k|}$, i.e., $i \sin(k_{in}|z_j - z_k|)$ is always zero, which changes the transmission of the Gaussian pulse dramatically. Moreover, we give the transmission, reflection, and loss as a function of the driving field Ω_c , as shown in Fig. 5(j). We observe that, as we enhance the driving field, the transmission increases from zero rapidly, and inversely, both the reflection and loss decrease to zero quickly. When the Rabi frequency of the driving field is large enough, for example, $\Omega_c = 3.5\Gamma'_e$, the transmission will approach 100%, and both the reflection and loss will touch zero. That is, by changing the driving field, we can effectively control the transport properties of the incident single-photon pulse, which is consistent with the results shown in Fig. 5(g).

Finally, we study the transmission, reflection, and loss

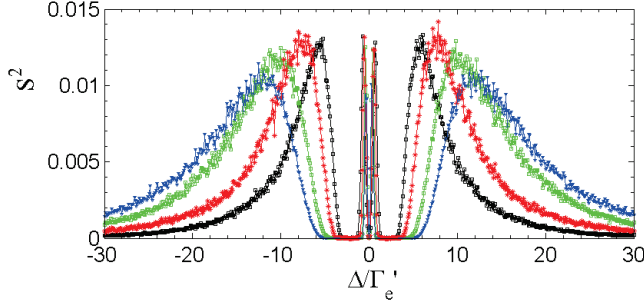


FIG. 6: The variance s^2 of the transmission T when $n=10$ (black line with squares), $n=20$ (red line with asterisks), $n=40$ (green line with circles), $n=60$ (blue line with down triangles) atoms are placed randomly over $N=200$ sites. Here, 1000 samples of atomic positions are averaged per detuning with $k_{in}d = \pi/2$, $\Omega_p = 0.001\Gamma'_e$, $\Omega_c = 2\Gamma'_e$, $\Gamma'_s = 0$, and $\Delta_c = 0$.

as a function of the filling factor n/N for two different choices of the driving fields with $N=50$. As shown in Fig. 5(k), when $\Omega_c = 2\Gamma'_e$, the transmission decreases slowly from 1 to a nonzero value as we add the number of the atoms, while for the reflection, it first increases from zero slowly and then decreases to zero slowly. Moreover, when the filling factor is small ($0 < n/N \leq 0.2$), the loss scales nonlinearly with the filling factor, when the filling factor is large ($0.2 < n/N \leq 1.0$), the loss scales linearly with the filling factor. For $\Omega_c = 0.5\Gamma'_e$ with other parameters remaining unchanged, the results are shown in Fig. 5(l). Similarly, the variation trends of the reflection, transmission, and loss with the filling factor are basically the same. Differently, we observe that, with the equal number of the atoms, both the loss and the reflection of the Gaussian pulse in this case are larger than that for $\Omega_c = 2\Gamma'_e$, while the transmission in this case becomes much smaller than that for $\Omega_c = 2\Gamma'_e$. In other words, the driving field influences the decay rate of the atoms out of the waveguide, i.e., the stronger the driving field, the weaker the loss, which is consistent with the results shown in Fig. 5(j).

C. The variance caused by the randomness of atomic positions

Different from the previous work where the atoms are equally located with a deterministic separation, we focus on the case that the atoms are randomly placed in a lattice along the waveguide. In our scheme, due to the various configurations of atomic positions, the scattering properties of single-photon pulse are variational. Here, to describe the influence on the transmission caused by the atomic positions, we use the variance s^2 , which is defined as

$$s^2 = \frac{1}{m} \sum_i^m (T_i - \bar{T})^2, \quad (13)$$

where m denotes the sample size of atomic positions, T_i is the transmission for the i^{th} sample, and \bar{T} is the average transmission for all samples.

As shown in Fig. 6, we obtain the variance s^2 of the transmission as a function of the detuning for 1000 samples when $n=10$ atoms are randomly placed in $N=200$ sites. We observe that the plot is symmetric, and s^2 is zero in a range of the frequency detuning around $\Delta = \pm\Omega_c$ and when $\Delta=0$, which is the result of EIT and the optical depth in transmission shown in Fig. 3(a)-(b). There are two peaks around the detuning $\Delta = \Omega_c$ ($\Delta = -\Omega_c$), i.e., when the detuning is shifted around $\Delta = \pm\Omega_c$, the influence of the atomic positions on transmission T become obvious. Moreover, s^2 will approach zero for a large detuning, which corresponds to the case that the photon pulse transmits the atomic ensemble with no interaction, and the transmission is not affected by the atomic positions. We also study the variance s^2 of the transmission T for different choices of the number of the atoms. Here, we consider another three cases, i.e., the number of atoms is $n=20, 40, 60$, respectively. We see that the width of the dip near the Rabi frequency of the driving field is determined by the number of the atoms when the sites of lattice N is fixed. In detail, as we add the number of the atoms, the width of the dip around the Rabi frequency of the driving field increases. Moreover, for the region of the detuning $12 \leq |\Delta|/\Gamma'_e \leq 30$, when we increase the number of the atoms, the value of the variance s^2 becomes larger. The results show that more atoms bring more fluctuation on the transmitted spectrum for a fixed sites N of the lattice.

D. Two-photon correlation

The main signature of non-classical light is that the photon can be bunched or anti-bunched, which can be calculated by photon-photon correlation function $g^{(2)}$ (also called the second-order coherence [47]). For a steady state, $g^{(2)}$ of the output field is defined as

$$g^{(2)}(\tau) = \lim_{t \rightarrow \infty} \frac{\langle a^\dagger(z, t) a^\dagger(z, t + \tau) a(z, t + \tau) a(z, t) \rangle}{\langle a^\dagger(z, t) a(z, t) \rangle \langle a^\dagger(z, t + \tau) a(z, t + \tau) \rangle}. \quad (14)$$

In our system, we can switch this definition to the Schrödinger picture:

$$g_\alpha^{(2)}(\tau) = \frac{\langle \psi | a_\alpha^\dagger(z) e^{iH\tau} a_\alpha^\dagger(z) a_\alpha(z) e^{-iH\tau} a_\alpha(z) | \psi \rangle}{|\langle \psi | a_\alpha^\dagger(z) a_\alpha(z) | \psi \rangle|^2}, \quad (15)$$

where $|\psi\rangle$ is the steady-state wavevector, and $\alpha=R, T$.

The two-photon correlation functions for two-level and three-level atoms coupled to an infinite waveguide have been considered in the previous work [38, 45, 48, 49]. Now, with a weak probe field ($\Omega_p \ll \Gamma'_e$), we discuss photon-photon correlation function $g^{(2)}$ for two choices of the driving fields in the off-resonant case when $n=10$

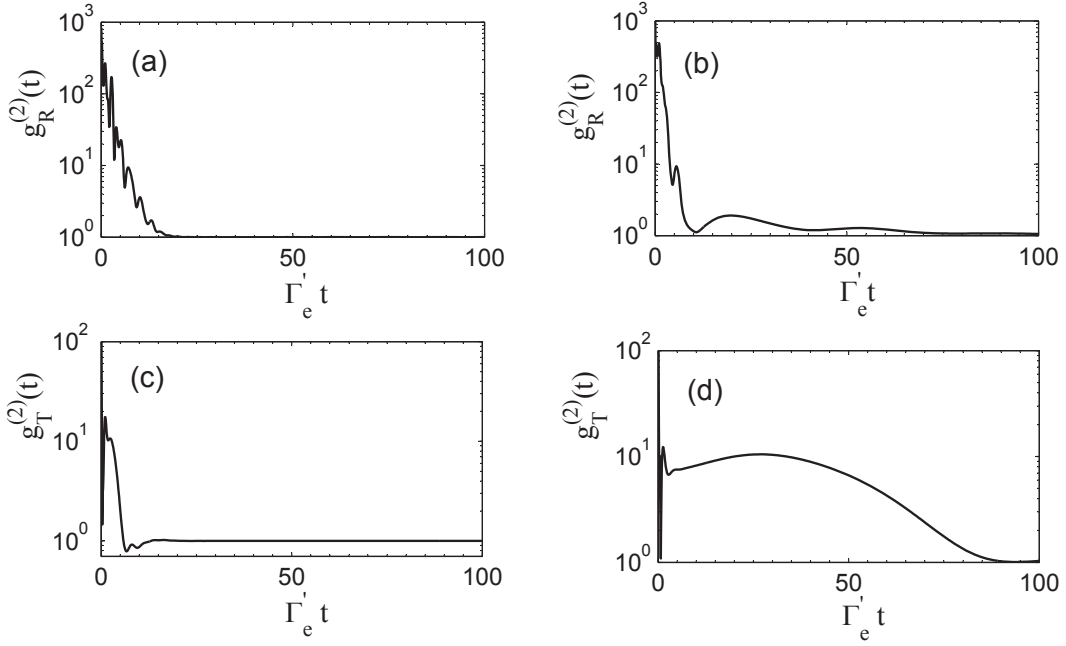


FIG. 7: The photon-photon correlation function $g^{(2)}(t)$ of the output field when $n = 10$ atoms are placed randomly over $N = 200$ sites. The first row is for transmitted field with the driving field (a) $\Omega_c = 2\Gamma'_e$, and (b) $\Omega_c = 0.5\Gamma'_e$. The second row is for reflected field with the driving field (c) $\Omega_c = 2\Gamma'_e$, and (d) $\Omega_c = 0.5\Gamma'_e$. Here, the frequency of the incident photons is chosen as one of the frequencies for $T = R$, and we average 1000 samples of atomic positions with $\Omega_p = 0.001\Gamma'_e$, $k_{in}d = \pi/2$, $\Delta_c = 0$, and $\Gamma'_s = 0$.

three-level atoms are randomly placed over $N = 200$ sites. Here, the frequencies of the two identical photons are chosen as one of the frequencies for $T = R$, which are labeled by blue lines in Figs. 3(a)-(b). As shown in Fig. 7, we observe that strong initial bunching ($g^{(2)} > 1$) is present for both reflection and transmission. Differently, as the time $\Gamma_{1D}t$ increases, bunching dominates at all times with quantum beats (oscillation) for reflection $g_R^{(2)}$ with two different driving fields $\Omega_c = 2\Gamma'_e$ and $\Omega_c = 0.5\Gamma'_e$, while for transmission $g_T^{(2)}$, when $\Omega_c = 2\Gamma'_e$, the initial bunching is followed by anti-bunching ($g^{(2)} < 1$) with a small region of the parameter $\Gamma'_e t$, as shown in Fig. 7(c), when $\Omega_c = 0.5\Gamma'_e$, no anti-bunching appears in the reflected field, which is shown in Fig. 7(d). Moreover, the intensity of the driving field Ω_c has an obvious influence on the correlations properties. By comparing the first and second columns of Fig. 7, we find that, for both the transmitted and reflected fields, when we enhance the driving field, the timescale for the decay of the two-photon correlations will be considerably shortened with more oscillations.

Specifically, on resonance $\Delta = 0$, since the incident photons can transmit the atomic ensemble with 100%, no correlation will be generated. The correlation function of the transmitted field is $g_T^{(2)} = 1$ (not shown), which is consistent with the results in Refs. [35, 50]. Actually, this phenomenon is known as "fluorescence quenching" [51, 52] and is not influenced by the parameters of our

system, such as the number of the atoms, the driving field, lattice constant d , and the atomic positions. The above calculations show that our system may provide an effective candidate for producing non-classical light in experiment.

IV. CONCLUSION

In summary, with an effective non-Hermitian Hamiltonian, we have studied the interaction between a single photon and an ensemble of Λ -type three-level atoms coupled to a 1D waveguide. Different from the previous work where the atoms are equally spaced, in our scheme, the atoms are randomly located in the lattice along the axis of the 1D waveguide, which closely corresponds to the practical condition that the atomic positions can not be controlled precisely in experiment due to inevitable technological spreading of the parameters. Since the transport properties is fluctuant with the various configurations of the atomic positions and single-shot spectrum is often not available because of finite trap lifetimes, we adopt the average optical properties from a large sample of the atomic positions.

Assuming that the incident photon is a plane wave with single frequency, we first calculate the transmission and reflection spectrums, concluding that the scattering properties of our system are quite different from the case that the atoms are equally spaced with a deterministic sepa-

ration. Then, we adopt a photon with Gaussian shape as the incident pulse, and analyse the rich optical properties with the parameters, such as the number of the atoms, the driving field, lattice constant d , and coupling strength Γ_{1D} . Our system may find application in quantum information technology, such as a single-photon frequency filter. We also study the variance of the transmission caused by the atomic positions, which exhibits different influence of atomic positions on the scattering properties with different detuning. Moreover, we calculate the photon-photon correlation of the output fields generated by the scattering between photons and atomic ensemble coupled to the 1D waveguide, which shows non-classical behavior such as bunching and anti-bunching. That is, the scattering between a single photon and atomic en-

semble may provide an effective method for generating non-classical light in experiment.

ACKNOWLEDGMENTS

GZS, FGD and GJY are supported by the National Natural Science Foundation of China under Grants No. 11474026 and No. 11674033, and the Fundamental Research Funds for the Central Universities under Grant No. 2015KJJCA01. EM, WN and LCK acknowledge support from the National Research Foundation and Ministry of Education, Singapore.

-
- [1] H. J. Kimble, *Nature (London)* **453**, 1023 (2008).
 - [2] H. Mabuchi and A. C. Doherty, *Science* **298**, 1372 (2002).
 - [3] H. Walther, B. T. H. Varcoe, B. G. Englert, and T. Becker, *Rep. Prog. Phys.* **69**, 1325 (2006).
 - [4] J. T. Shen and S. Fan, *Opt. Lett.* **30**, 2001 (2005).
 - [5] J. T. Shen and S. Fan, *Phys. Rev. Lett.* **95**, 213001 (2005).
 - [6] J. T. Shen and S. Fan, *Phys. Rev. A* **76**, 062709 (2007).
 - [7] A. V. Akimov, A. Mukherjee, C. L. Yu, D. E. Chang, A. S. Zibrov, P. R. Hemmer, H. Park, and M. D. Lukin, *Nature (London)* **450**, 402 (2007).
 - [8] J. T. Shen and S. Fan, *Phys. Rev. Lett.* **98**, 153003 (2007).
 - [9] T. S. Tsoi and C. K. Law, *Phys. Rev. A* **78**, 063832 (2008).
 - [10] L. Zhou, Z. R. Gong, Y. X. Liu, C. P. Sun, and F. Nori, *Phys. Rev. Lett.* **101**, 100501 (2008).
 - [11] T. S. Tsoi and C. K. Law, *Phys. Rev. A* **80**, 033823 (2009).
 - [12] M. Bajcsy, S. Hofferberth, V. Balic, T. Peyronel, M. Hafezi, A. S. Zibrov, V. Vuleticand, and M. D. Lukin, *Phys. Rev. Lett.* **102**, 203902 (2009).
 - [13] P. Longo, P. Schmittechert, and K. Busch, *Phys. Rev. Lett.* **104**, 023602 (2010).
 - [14] D. Witthaut and A. S. Sørensen, *New J. Phys.* **12**, 043052 (2010).
 - [15] O. Astafiev, A. M. Zagoskin, A. A. Abdumalikov, Y. A. Pashkin, T. Yamamoto, K. Inomata, Y. Nakamura, and J. S. Tsai, *Science* **327**, 840 (2010).
 - [16] T. M. Babinec, J. M. Hausmann, M. Khan, Y. Zhang, J. R. Maze, P. R. Hemmer, and M. Lončar, *Nat. Nanotechnol.* **5**, 195 (2010).
 - [17] H. Zheng, D. J. Gauthier, and H. U. Baranger, *Phys. Rev. Lett.* **107**, 023601 (2011).
 - [18] D. Roy, *Phys. Rev. Lett.* **106**, 053601 (2011).
 - [19] J. Bleuse, J. Claudon, M. Creasey, N. S. Malik, J. M. Gérard, I. Maksymov, J. P. Hugonin, and P. Lalanne, *Phys. Rev. Lett.* **106**, 103601 (2011).
 - [20] M. Bradford, K. C. Obi, and J. T. Shen, *Phys. Rev. Lett.* **108**, 103902 (2012).
 - [21] M. Pletyukhov and V. Gritsev, *New J. Phys.* **14**, 095028 (2012).
 - [22] B. Dayan, A. S. Parkins, T. Aoki, E. P. Ostby, K. J. Vahala, and H. J. Kimble, *Science* **319**, 1062 (2013).
 - [23] H. Zheng and H. U. Baranger, *Phys. Rev. Lett.* **111**, 090502 (2013).
 - [24] D. Roy, *Sci. Rep.* **3**, 2337 (2013).
 - [25] A. González-Tudela, C. L. Hung, D. E. Chang, J. I. Cirac, and H. J. Kimble, *Nat. Photon.* **9**, 320 (2015).
 - [26] Y. S. Greenberg and A. A. Shtygashev, *Phys. Rev. A* **92**, 063835 (2015).
 - [27] A. Wallraff, D. I. Schuster, A. Blais, L. Frunzio, R. S. Huang, J. Majer, S. Kumar, S. M. Girvin, and R. J. Schoelkopf, *Nature (London)* **431**, 162 (2004).
 - [28] O. Astafiev, A. M. Zagoskin, A. Abdumalikov, Y. A. Pashkin, T. Yamamoto, K. Inomata, Y. Nakamura, and J. Tsai, *Science* **327**, 840 (2010).
 - [29] I. C. Hoi, C. M. Wilson, G. Johansson, T. Palomaki, B. Peropadre, and P. Delsing, *Phys. Rev. Lett.* **107**, 073601 (2011).
 - [30] L. H. Frandsen, A. V. Lavrinenko, J. Fage-Pedersen, and P. I. Borel, *Opt. Express* **14**, 9444 (2006).
 - [31] J. Claudon, J. Bleuse, N. S. Malik, M. Bazin, P. Jaffrennou, N. Gregersen, C. Sauvan, P. Lalanne, and J. M. Gérard, *Nat. Photon.* **4**, 174 (2010).
 - [32] S. Fan, S. E. Kocabas, and J. T. Shen, *Phys. Rev. A* **82**, 063821 (2010).
 - [33] J. F. Huang, T. Shi, C. P. Sun, and F. Nori, *Phys. Rev. A* **88**, 013836 (2013).
 - [34] Y. Chen, M. Wubs, J. Mørk, and A. F. Koenderink, *New J. Phys.* **13**, 103010 (2011).
 - [35] D. Roy and N. Bondyopadhyaya, *Phys. Rev. A* **89**, 043806 (2014).
 - [36] Z. Liao, X. Zeng, S. Y. Zhu, and M. S. Zubairy, *Phys. Rev. A* **92**, 023806 (2015).
 - [37] E. Munro, L. C. Kwek, and D. E. Chang, *arXiv:1604.02893v2 [quant-ph]*.
 - [38] H. Zheng and H. U. Baranger, *Phys. Rev. Lett.* **110**, 113601 (2013).
 - [39] J. T. Shen and S. Fan, *Phys. Rev. A* **79**, 023837 (2009).
 - [40] H. J. Carmichael, *An Open Systems Approach to Quantum Optics* (Springer, Berlin, 1993).
 - [41] T. Caneva, M. T. Manzoni, T. Shi, J. S. Douglas, J. I. Cirac, and D. E. Chang, *New J. Phys.* **17**, 113001 (2015).
 - [42] P. M. Leung and B. C. Sanders, *Phys. Rev. Lett.* **109**, 253603 (2012).

- [43] M. Fleischhauer, A. Imamoglu, and J. P. Marangos, Rev. Mod. Phys. **77**, 633 (2005).
- [44] P. Lambropoulos and D. Petrosyan, *Fundamentals of Quantum Optics and Quantum Information* (Springer, Berlin, 2006).
- [45] Y. L. L. Fang and H. U. Baranger, Physica E **78**, 92 (2016).
- [46] P. Kolchin, C. Belthangady, S. Du, G. Y. Yin, and S. E. Harris, Phys. Rev. Lett. **101**, 103601 (2008).
- [47] R. Loudon, The Quantum Theory of Light, 3rd edition, Oxford University Press, New York, 2003.
- [48] M. Laakso and M. Pletyukhov, Phys. Rev. Lett. **113**, 183601 (2014).
- [49] Y. L. L. Fang and H. U. Baranger, Phys. Rev. A **91**, 053845 (2015).
- [50] H. Zheng, D. J. Gauthier, and H. U. Baranger, Phys. Rev. A **85**, 043832 (2012).
- [51] P. Zhou and S. Swain, Phys. Rev. Lett. **77**, 3995-3998 (1996).
- [52] E. Rephaeli, Ş. E. Kocabaş, and S. Fan, Phys. Rev. A **84**, 063832 (2011).